

Adversarial Attacks on Binary Image Recognition Systems

Eric Balkanski^{1,2} Harrison Chase¹ Kojin Oshiba¹

Alexander Rilee¹ Yaron Singer^{1,3} Richard Wang¹

¹*Robust Intelligence* ²*Columbia University* ³*Harvard University*

Abstract

We initiate the study of adversarial attacks on models for binary (i.e. black and white) image classification. Although there has been a great deal of work on attacking models for colored and grayscale images, little is known about attacks on models for binary images. Models trained to classify binary images are used in text recognition applications such as check processing, license plate recognition, invoice processing, and many others. In contrast to colored and grayscale images, the search space of attacks on binary images is extremely restricted and noise cannot be hidden with minor perturbations in each pixel. Thus, the optimization landscape of attacks on binary images introduces new fundamental challenges.

In this paper we introduce a new attack algorithm called SCAR, designed to fool classifiers of binary images. We show that SCAR significantly outperforms existing L_0 attacks applied to the binary setting and use it to demonstrate the vulnerability of real-world text recognition systems. SCAR's strong performance in practice contrasts with hardness results that show the existence of classifiers that are provably robust to large perturbations. In many cases, altering a single pixel is sufficient to trick Tesseract, a popular open-source text recognition system, to misclassify a word as a different word in the English dictionary. We also license software from providers of check processing systems to most of the major US banks and demonstrate the vulnerability of check recognitions for mobile deposits. These systems are substantially harder to fool since they classify both the handwritten amounts in digits and letters, independently. Nevertheless, we generalize SCAR to design attacks that fool state-of-the-art check processing systems using unnoticeable perturbations that lead to misclassification of deposit amounts. Consequently, this is a powerful method to perform financial fraud.

1 Introduction

In this paper we study adversarial attacks on models designed to classify binary (i.e. black and white) images. Models for binary image classification are heavily used across a variety of applications that include receipt processing, passport recognition, check processing, and license plate recognition, just to name a few. In such applications, the text recognition system typically binarizes the input image (e.g. check processing [13], document extraction [10]) and trains a model to classify binary images.

In recent years there has been an overwhelming interest in understanding the vulnerabilities of AI systems. In particular, a great deal of work has designed attacks on image classification models (e.g. [29, 8, 21, 14, 23, 19, 3, 4, 11, 12, 30, 9, 18]). Such attacks distort images in a manner that is virtually imperceptible to the human eye and yet cause state-of-the-art models to misclassify these images. Although there has been a great deal of work on attacking image classification models, these attacks are designed for colored and grayscale images. These attacks hide the noise in the distorted images by making minor perturbations in the color values of each pixel.

Somewhat surprisingly, when it comes to binary images, the vulnerability of state-of-the-art models is poorly understood. In contrast to colored and grayscale images, the search space of attacks on binary images is extremely restricted and noise cannot be hidden with minor perturbations of color values in each pixel. As a result, existing attack algorithms on machine learning systems do not apply to binary inputs. Since binary image classifiers are used in high-stakes decision making and are heavily used in banking and other multi-billion dollar industries, the natural question is:

Are models for binary image classification used in industry vulnerable to adversarial attacks?

In this paper we initiate the study of attacks on binary image classifiers. We develop an attack algorithm, called SCAR, designed to fool binary image classifiers. SCAR carefully selects pixels to flip to the opposite color in a query efficient manner, which is a central challenge when attacking black-box models.

We first show that SCAR outperforms existing attacks that we apply to the binary setting on multiple models trained over the MNIST and EMNIST datasets, as well as models for handwritten strings and printed word recognition. The most relevant attacks for binary images are L_0 attacks which minimize the number of pixels in which the distorted image differs from the original image [23, 3, 26, 9]. We then use SCAR to demonstrate the vulnerability of text recognition systems used in industry. We fool commercial check processing systems used by most of the major US banks for mobile check deposits. One major challenge in attacking these systems, whose software we licensed from providers, is that there are two independent classifiers, one for the amount written in words and one for the amount written in numbers, that must be fooled with the same wrong amount. Check fraud is a major concern for US banks, accounting for \$1.3 billion in losses in 2018 [2]. Since check fraud occurs at large scale, we believe that the vulnerability of check processing systems to adversarial attacks raises a serious concern.

We also show that no attack can obtain reasonable guarantees on the number of pixel inversions needed to cause misclassification as there exist simple classifiers that are provably robust to even large perturbations. There exist classifiers for d -dimensional binary images such that every class contains some image that requires $\Omega(d)$ pixel inversions (L_0 distance) to change the label of that image and such that for every class, a random image in that class requires $\Omega(\sqrt{d})$ pixel inversions in expectation.

Related work. The study of adversarial attacks was initiated in the seminal work by Szegedy et al. [29] that showed that models for image classification are susceptible to minor perturbations in the input. There has since then been a long line of work developing attacks on colored and grayscale images. Most relevant to us are L_0 attacks, which iteratively make minor perturbations in carefully chosen pixels to minimize the total number of pixels that have been modified [23, 3, 26, 9]. We compare our attack to two L_0 attacks that are applicable in the black-box binary setting [26, 9]. Another related area of research focuses on developing attacks that query the model as few times as possible [4, 11, 12, 9, 18, 30, 1]. We discuss below why most of these attacks cannot be applied to the binary setting. There has been previous work on attacking OCR systems [28], but the setting deals with grayscale images and white-box access to the model.

Attacks on colored and grayscale images employ continuous optimization techniques and are fundamentally different than attacks on binary images which, due to the binary nature of each pixel, employ combinatorial optimization approaches. Previous work has formulated adversarial attack settings as combinatorial optimization problems, but in drastically different settings. Lei et al. [17] consider attacks on text classification for tasks such as sentiment analysis and fake news detection, which is a different domain than OCR. Moon et al. [20] formulate L_∞ attacks on colored image classification as a combinatorial optimization problem where the search space for the change in each pixel is $\{-\varepsilon, \varepsilon\}$ instead of $[-\varepsilon, \varepsilon]$.

Finally, we also note that binarization, i.e. transforming colored or grayscale images into black and white images, has been studied as a technique to improve the robustness of models, especially to L_2 and L_∞ attacks [26, 25, 7].

Previous attacks are ineffective in the binary setting. Previous attacks on classifiers for grayscale and colored images are not directly applicable to classifiers for binary images. These attacks iteratively cause small perturbations in the pixel values. Small changes in the pixel values of binary images are not possible since there are only two possible values.

One potential approach to extend previous attacks to the binary setting is to relax the binary pixel values to be in the grayscale range and run an attack over this relaxed domain. The issue with this approach is that binary image classifiers only take as input binary images and small changes in the relaxed grayscale domain are lost when rounding the pixel values back to being binary.

Another potential approach is to increase the step size of an attack such that a small change in the pixel value of a grayscale or colored image instead causes the pixel value of a binary image to flip. For gradient-based attacks, which cause minor perturbations in all pixels, this causes a large number of pixel flips. This approach is more relevant for L_0 attacks since they perturb a smaller number of pixels. There are two L_0 attacks which can be applied to the binary setting with this approach. The first is SIMBA [9] which modifies a single pixel at each iteration and the second is POINTWISE [26], which first applies random salt and pepper noise until the image is misclassified and then greedily returns each modified pixels to its original color if the image remains misclassified. However, even these L_0 attacks extended to the binary setting result in a large and visible number of pixel inversions, as shown in the experiments in Section 6.

2 Problem Formulation

Binary images. We consider binary images $\mathbf{x} \in \{0, 1\}^d$, which are d -dimensional images such that each pixel is either black (value 0) or white (value 1). An m -class classifier F maps \mathbf{x} to

a probability distribution $F(\mathbf{x}) \in [0, 1]^m$ where $F(\mathbf{x})_i$ corresponds to the confidence that image \mathbf{x} belongs to class i . The predicted label y of \mathbf{x} is the class with the highest confidence, i.e., $y = \arg \max_i F(\mathbf{x})_i$.

OCR systems. Optical Character Recognition (OCR) systems convert images of handwritten or printed text to strings of characters. Typically, a preprocessing step of OCR systems is to convert the input to a binary format. To formalize the problem of attacking OCR systems, we consider a classifier F where the labels are strings of characters. Given a binary image \mathbf{x} with label y , we wish to produce an adversarial example \mathbf{x}' which is similar to \mathbf{x} , but has a predicted label $y' \neq y$. For example, given an image \mathbf{x} of license plate 23FC6A, our goal is to produce a similar image \mathbf{x}' that is recognized as a different license plate number. We measure the similarity of an adversarial image \mathbf{x}' to the original image \mathbf{x} with a perceptibility metric $D_{\mathbf{x}}(\mathbf{x}')$. For binary images, a natural metric is the number of pixels where \mathbf{x} and \mathbf{x}' differ, which corresponds to the L_0 distance between the two images. Finding an adversarial example can thus be formulated as the following optimization problem:

$$\min_{\substack{\mathbf{x}' \in \{0,1\}^d \\ \|\mathbf{x} - \mathbf{x}'\|_0 \leq k}} F(\mathbf{x}')_y$$

where k is the maximum dissimilarity tolerated for adversarial image \mathbf{x}' . For targeted attacks with target label y_t , we instead maximize $F(\mathbf{x}')_{y_t}$. Since there are at least $\binom{d}{k}$ feasible solutions for \mathbf{x}' , which is exponential in k , this is a computationally hard problem.

Check processing systems. A check processing system F accepts as input a binary image \mathbf{x} of a check and outputs confidence scores $F(\mathbf{x})$ which represent the most likely amounts that the check is for. Check processing systems are a special family of OCR systems that consist of two independent models that verify each other. Models F_C and F_L for Courtesy and Legal Amount Recognition (CAR and LAR) classify the amounts written in numbers and in words respectively. If the predicted labels of the two models do not match, the check is flagged. For example, if the CAR of a valid check reads 100, and the LAR reads “one hundred”, the two values match and the check is processed. The main challenge with attacking check processing systems over an input \mathbf{x} is to craft an adversarial example \mathbf{x}' with the same target label for both F_C and F_L . Returning to the previous example, a successful adversarial check image might have the CAR read 900 and the LAR read “nine hundred”. For this targeted attack, the optimization problem is:

$$\begin{aligned} \max_{\substack{\mathbf{x}' \in \{0,1\}^d, y_t \neq y \\ \|\mathbf{x} - \mathbf{x}'\|_0 \leq k}} & F_C(\mathbf{x}')_{y_t} + F_L(\mathbf{x}')_{y_t} \\ \text{subject to} & y_t = \arg \max_i F_C(\mathbf{x}')_i = \arg \max_i F_L(\mathbf{x}')_i \end{aligned}$$

The attacker first needs to select a target amount y_t different from the true amount y , and then attack F_C and F_L such that both misclassify \mathbf{x}' as amount y_t . Since check processing systems also flag checks for which the models have low confidence in their predictions, we want to maximize both the probabilities $F_C(\mathbf{x}')_{y_t}$ and $F_L(\mathbf{x}')_{y_t}$. In order to have \mathbf{x}' look as similar to \mathbf{x} as possible, we also limit the number of modified pixels to be at most k . Check processing systems are configured such that F_C and F_L only output the probabilities for a limited number of their most probable amounts. This limitation makes the task of selecting a target amount challenging, as aside from the true amount, the most probable amounts for each of F_C and F_L may be disjoint sets.

Black-box access. We assume that we do not have any information about the OCR model F and can only observe its outputs, which we formalize with the score-based black-box setting where an attacker only has access to the output probability distributions of a model F over queries \mathbf{x}' .

3 Existence of Provably Robust Classifiers for Binary Images

Before presenting the attacks, we first show the existence of simple binary image classifiers that are provably robust to any attack that modifies a large, bounded, number of pixels. This implies that there is no attack that can obtain reasonable guarantees on the number of pixel inversions (L_0 distance) needed to cause misclassification.

We show such results for two different settings. First, there exists an m -class linear classifier F for d -dimensional binary images such that every class contains some image whose predicted label according to F cannot be changed with $o(d)$ pixel flips, i.e., every class contains at least one image which requires a number of pixel flips that is linear in the total number of pixels to be attacked. The analysis uses a probabilistic argument and is deferred to the appendix.

Theorem 1. *There exists an m -class linear classifier F for d -dimensional binary images s.t. for all classes i , there exists at least one binary image \mathbf{x} in i that is robust to $d/4 - \sqrt{2d \log m}/2$ pixel changes, i.e., for all \mathbf{x}' s.t. $\|\mathbf{x} - \mathbf{x}'\|_0 \leq d/4 - \sqrt{2d \log m}/2$, $\arg \max_j F(\mathbf{x}')_j = i$.*

This robustness result holds for all m classes, but only for the most robust image in each class. We also show the existence of a classifier robust to attacks on an image drawn uniformly at random. There exists a 2-class classifier such that for both classes, a uniformly random image in that class requires, in expectation, $\Omega(\sqrt{d})$ pixel flips to be attacked. The analysis relies on anti-concentration bounds and is deferred to the appendix as well.

Theorem 2. *There exists a 2-class linear classifier F for d -dimensional binary images such that for both classes i , a uniformly random binary image \mathbf{x} in that class i is robust to $\sqrt{d}/8$ pixel changes in expectation, i.e. $\mathbb{E}_{\mathbf{x} \sim \mathcal{U}(i)}[\min_{\mathbf{x}': \arg \max_j F(\mathbf{x}')_j \neq i} \|\mathbf{x} - \mathbf{x}'\|_0] \geq \sqrt{d}/8$.*

These hardness results hold for worst-case classifiers. Experimental results in Section 6 show that, in practice, classifiers for binary images are highly vulnerable and that the algorithms that we present next require a small number of pixel flips to cause misclassification.

4 Attacking Binary Images

In this section, we present SCAR, our main attack algorithm. We begin by describing a simplified version of SCAR, Algorithm 1, then discuss the issues of hiding noise in binary images and optimizing the number of queries, and finally describe SCAR. At each iteration, Algorithm 1 finds the pixel p in input image \mathbf{x} such that flipping x_p to the opposite color causes the largest decrease in $F(\mathbf{x}')_y$, which is the confidence that this perturbed input \mathbf{x}' is classified as the true label y . It flips this pixel and repeats this process until either the perturbed input is classified as label $y' \neq y$ or the maximum L_0 distance k with the original image is reached. Because binary images \mathbf{x} are such that $\mathbf{x} \in \{0, 1\}^d$, we implicitly work in \mathbb{Z}_2^d . In particular, with $\mathbf{e}_1, \dots, \mathbf{e}_d$ as the standard basis vectors, $\mathbf{x}' + \mathbf{e}_p$ represents the image \mathbf{x}' with pixel p flipped.

Algorithm 1 A combinatorial attack on OCR systems.

Input: model F , image \mathbf{x} , label y
 $\mathbf{x}' \leftarrow \mathbf{x}$
while $y = \arg \max_i F(\mathbf{x}')_i$ and $\|\mathbf{x}' - \mathbf{x}\|_0 \leq k$ **do**
 $p' \leftarrow \arg \min_p F(\mathbf{x}' + \mathbf{e}_p)_y$
 $\mathbf{x}' \leftarrow \mathbf{x}' + \mathbf{e}_{p'}$
return \mathbf{x}'

Although the adversarial images produced by Algorithm 1 successfully fool models and have small L_0 distance to the original image, it suffers in two aspects: the noise added to the inputs is visible to the human eye, and the required number of queries to the model is large.

Hiding the noise. Attacks on images in a binary domain are fundamentally different from attacks on colored or grayscale images. In the latter two cases, the noise is often imperceptible because the change to any individual pixel is small relative to the range of possible colors. Since attacks on binary images can only invert a pixel’s color or leave it untouched, noisy pixels are highly visible if their colors contrast with that of their neighboring pixels. This is a shortcoming of Algorithm 1, which results in noise with small L_0 distance but that is highly visible (for example, see Figure 1). To address this issue, we impose a new constraint which only allows modifying pixels on the *boundary* of black and white regions in the image. A pixel is on a boundary if it is white and at least one of its eight neighboring pixels is black (or vice-versa). Adversarial examples produced under this constraint have a greater L_0 distance to their original images, but the noise is significantly less noticeable.

Optimizing the number of queries. An attack may be computationally expensive if it requires many queries to a black-box model. For paid services where a model is hidden behind an API, running attacks can be financially costly as well. Several works have proposed techniques to reduce the number of queries. Many of these are based on gradient estimation [4, 30, 11, 12, 1]. Recently, several gradient-free black-box attacks have also been proposed. Li et al. [18] and Moon et al. [20] propose two such approaches, but these rely on taking small steps of size ε in a direction which modifies *all* pixels. Taking small steps in some direction, whether with gradient estimation or gradient-free approaches, is not possible here since there are only two possible values for each pixel. SIMBA[9], another gradient-free attack, can be extended to the binary setting and is evaluated in the context of binary images in Section 6. We propose two optimization techniques to exploit correlations between pixels both spatially and temporally. We define the *gain* from flipping pixel p at point \mathbf{x}' as the following discrete derivative of F in the direction of p :

$$F(\mathbf{x}')_y - F(\mathbf{x}' + \mathbf{e}_p)_y$$

We say a pixel p has *large gain* if this value is larger than a threshold τ .

- **Spatial correlations.** Pixels in the same spatial regions are likely to have similar discrete derivatives (e.g. Figure 4 in appendix). At every iteration, we prioritize evaluating the gains of the eight pixels $N(p)$ neighboring the pixel p which was modified in the previous iteration of the algorithm. If one of these pixels has large gain, then we flip it and proceed to the next iteration without evaluating the remaining pixels.

- **Temporal correlations.** . Pixels with large discrete derivatives at one iteration are likely to also have large discrete derivatives in the next iteration (e.g. Figure 5 in appendix). At each iteration, we first consider pixels that had large gain in the previous iteration. If one of these pixels still produces large gain in the current iteration, we flip it and proceed to the next iteration without evaluating the remaining pixels.

Scar. In order to improve on the number of queries, SCAR (Algorithm 2) prioritizes evaluating the discrete derivatives at pixels which are expected to have large gain according to the spatial and temporal correlations. If one of these pixels has large gain, then it is flipped and the remaining pixels are not evaluated. If none of these pixels have large gain, we then consider all pixels on the boundary $B(\mathbf{x})$ of black and white regions in the image \mathbf{x} . In this set, the pixel with the largest gain is flipped regardless of whether it has gain greater than τ . As before, we denote the standard basis vector in the direction of coordinate i with \mathbf{e}_i . We keep track of the gain of each pixel with vector \mathbf{g} .

Algorithm 2 SCAR, Shaded Combinatorial Attack on Recognition systems.

Input: model F , image \mathbf{x} , label y , threshold τ , budget k

```

 $\mathbf{x}' \leftarrow \mathbf{x}, \mathbf{g} \leftarrow \mathbf{0}$ 
while  $y = \arg \max_i F(\mathbf{x}')_i$  and  $\|\mathbf{x}' - \mathbf{x}\|_0 \leq k$  do
  for  $p : g_p \geq \tau$  or  $p \in N(p')$  do
     $g_p \leftarrow F(\mathbf{x}')_y - F(\mathbf{x}' + \mathbf{e}_p)_y$ 
  if  $\max_p g_p < \tau$  then
    for  $p \in B(\mathbf{x}')$  do
       $g_p \leftarrow F(\mathbf{x}')_y - F(\mathbf{x}' + \mathbf{e}_p)_y$ 
   $p' \leftarrow \arg \max_p g_p$ 
   $\mathbf{x}' \leftarrow \mathbf{x}' + \mathbf{e}_{p'}$ 
return  $\mathbf{x}'$ 

```

Algorithm 2 is an untargeted attack which finds \mathbf{x}' which is classified as label $y' \neq y$ by F . It can easily be modified into a targeted attack with target label y_t by changing the first condition in the while loop from $y = \arg \max_i F(\mathbf{x}')_i$ to $y_t \neq \arg \max_i F(\mathbf{x}')_i$ and by computing the gains g_p as $F(\mathbf{x} + \mathbf{e}_p)_{y_t} - F(\mathbf{x})_{y_t}$ instead of $F(\mathbf{x})_y - F(\mathbf{x} + \mathbf{e}_p)_y$. Even though SCAR performs well in practice, we show in the appendix that there exists simple classifiers F for which SCAR requires, for most images \mathbf{x} , a linear number $k = O(d)$ of pixel flips to find an adversarial example \mathbf{x}' .

5 Simultaneous Attacks

There are two significant challenges to attacking check processing systems. In the previous section, we discussed the challenge caused by the preprocessing step that binarizes check images [13]. The second challenge is that check processing systems employ two independent models that verify the output of the other model: F_C classifies the amount written in numbers, and F_L classifies the amount written in letters. We thus propose an algorithm which tackles the problem of attacking two separate OCR systems simultaneously.

A natural approach is to search for a target amount at the intersection of what F_C and F_L determines are probable amounts. However, on unmodified checks, the models are often highly

confident of the true amount, and other amounts have extremely small probability, or do not even appear at all as predictions by the models.

To increase the likelihood of choosing a target amount which will result in an adversarial example, we first proceed with an untargeted attack on both F_C and F_L using SCAR, which returns image \mathbf{x}^u with reduced confidence in the true amount y . Then we choose the target amount y_t to be the amount i with the maximum value $\min(F_C(\mathbf{x}^u)_i, F_L(\mathbf{x}^u)_i)$, since our goal is to attack both F_C and F_L . Then we run T-SCAR, which is the targeted version of SCAR, twice to perform targeted attacks on both F_C and F_L over image \mathbf{x}^u .

Algorithm 3 The attack on check processing systems.

Input: check image \mathbf{x} , models F_C and F_L , label y
 $\mathbf{x}_C, \mathbf{x}_L \leftarrow$ extract CAR and LAR regions of \mathbf{x}
 $\mathbf{x}_C^u, \mathbf{x}_L^u \leftarrow$ SCAR(F_C, \mathbf{x}_C), SCAR(F_L, \mathbf{x}_L)
 $y_t \leftarrow \max_{i \neq y} \min(F_C(\mathbf{x}_C^u)_i, F_L(\mathbf{x}_L^u)_i)$
 $\mathbf{x}_C^t, \mathbf{x}_L^t \leftarrow$ T-SCAR(F_C, \mathbf{x}_C^u, y_t), T-SCAR(F_L, \mathbf{x}_L^u, y_t)
 $\mathbf{x}^t \leftarrow$ replace CAR, LAR regions of \mathbf{x} with $\mathbf{x}_C^t, \mathbf{x}_L^t$
return \mathbf{x}^t

6 Experiments

We demonstrate the effectiveness of SCAR for attacking text recognition systems. We attack, in increasing order of model complexity, standard models for single handwritten character classification (Section 6.2), an LSTM model for handwritten numbers classification (Section 6.3), a widely used open source model for typed text recognition called Tesseract (Section 6.4), and finally commercial check processing systems used by banks for mobile check deposit (Section 6.5).

6.1 Experimental setup

Benchmarks. We compare four attack algorithms.

- **Scar**, which is Algorithm 2 with threshold $\tau = 0.1$.
- **Vanilla-Scar**, which is Algorithm 1. We compare SCAR to Algorithm 1 to demonstrate the importance of hiding the noise and optimizing the number of queries.
- **SimBA**, which is Algorithm 1 in [9] with the Cartesian basis and $\varepsilon = 1$. SIMBA is an algorithm for attacking (colored) images in black-box settings using a small number of queries. At every iteration, it samples a direction \mathbf{q} and takes a step towards $\varepsilon\mathbf{q}$ or $-\varepsilon\mathbf{q}$ if one of these improves the objective. In the setting where \mathbf{q} is sampled from the Cartesian basis and $\varepsilon = 1$, SIMBA corresponds to an L_0 attack on binary images which iteratively chooses a random pixel and flips it if doing so results in a decrease in the confidence of the true label.
- **Pointwise** [26] first applies random salt and pepper noise until the image is misclassified. It then greedily returns each modified pixel to its original color if the image remains misclassified. We use the implementation of this attack available in Foolbox [24].

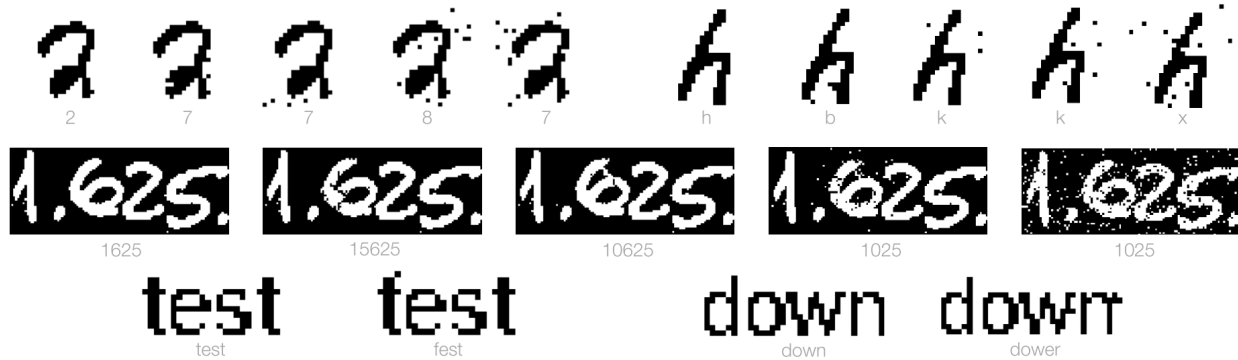


Figure 1: Examples of attacks on a CNN trained over MNIST (top left), a CNN trained over EMNIST (top right), an LSTM for handwritten numbers (center), and Tesseract for typed words (bottom). The images correspond to, from left to right, the original image, the outputs of SCAR, VANILLA-SCAR, POINTWISE, and SIMBA. The predicted labels are in light gray below each image. For Tesseract attacks (bottom), we show the original image and SCAR’s output.

Metrics. To evaluate the performance of each attack A over a model F and test set X , we use three metrics.

- The **success rate** of A is the fraction of images $\mathbf{x} \in X$ for which the output image $\mathbf{x}' = A(\mathbf{x})$ is adversarial, i.e. the predicted label y' of \mathbf{x}' is different from the true label y of \mathbf{x} . We only attack images \mathbf{x} which are initially correctly classified by F .
- We use the **L_0 distance** to measure how similar an image $\mathbf{x}' = A(\mathbf{x})$ is to the original image \mathbf{x} , which is the number of pixels where \mathbf{x} and \mathbf{x}' differ.
- The **number of queries** to model F to obtain output image $\mathbf{x}' = A(\mathbf{x})$.

The distance constraint k . Because the image dimension d differs for each experiment, we seek a principled approach to selecting the maximum L_0 distance k . For an image \mathbf{x} with label y , the L_0 constraint is

$$k = \alpha \cdot \frac{\mathcal{F}(\mathbf{x})}{|y|},$$

where $\mathcal{F}(\mathbf{x})$ counts the number of pixels in the foreground of the image, $\alpha \in [0, 1]$ is a fixed fraction, and $|y|$ represents the number of characters in y , e.g. $|23FC6A| = 6$. In other words, k is a fixed fraction of the average number of pixels per character in \mathbf{x} . In our experiments, we set $\alpha = \frac{1}{5}$.

6.2 Digit and character recognition systems

For each experiment, we provide further details about the datasets and models in the appendix.

The dataset. We train models over binarized versions of the MNIST digit [16] and EMNIST letter [5] datasets. We binarize each dataset with the map $x \mapsto \lfloor \frac{x}{128} \rfloor$. We additionally preprocess the EMNIST letter dataset to only include lowercase letters, since an uppercase letter which is misclassified as the corresponding lowercase letter does not change the semantic meaning of the

overall word. We randomly select 10 correctly-classified samples from each class in MNIST and EMNIST lowercase letters to form two datasets to attack.

Models. We consider five models, trained in the same manner for the MNIST and EMNIST datasets. Their Top-1 accuracies are given in Table 1.

Model	MNIST (Top-1 accuracy)	EMNIST (Top-1 accuracy)
LogReg	0.919	0.809
MLP2	0.980	0.934
CNN	0.990	0.950
LeNet5	0.990	0.943
SVM	0.941	0.875

Table 1: The Top-1 accuracies of a logistic regression model, a 2-layer perceptron, a convolutional neural network, a neural network from [15], and a support vector machine trained and evaluated over the MNIST and EMNIST datasets.

Results. We discuss the results of the attacks on the CNN model trained over MNIST and on the LeNet5 model trained over EMNIST, which are representative cases of the results for neural network models. The full results for the remaining 8 models are in the appendix.

In Figure 2, we observe that for fixed L_0 distances $\kappa \leq k$, VANILLA-SCAR has the highest success rate on the CNN model, i.e. the largest number of successful attacks with an L_0 distance at most κ . For example, 80% of the images were successfully attacked by flipping at most 7 of the 784 pixels of an MNIST image. SCAR’s success rate by L_0 distance is very close to VANILLA-SCAR, but enjoys two main advantages: first, the number of queries needed for these attacks is significantly smaller. Second, as shown in Figure 1, even though the L_0 distance is slightly larger than VANILLA-SCAR, the noise is less visible. SIMBA requires very few queries to obtain a success rate close to 40% and 65% respectively on the CNN and LeNet5, but this attack results in images with large L_0 distances. The success rate of this attack does not increase past 40% and 65% with a larger number of queries because the noise constraint k is reached. POINTWISE obtains a success rate close to 85% and 98% on the CNN and LeNet5, respectively. The average L_0 distance of the images produced by POINTWISE is between SCAR and SIMBA. Overall, SCAR obtains the best number of queries and L_0 distance combination. It is the only attack, together with VANILLA-SCAR, which consistently obtains a success rate close to 100 percent on MNIST and EMNIST models.

6.3 LSTM on handwritten numbers

The dataset. We train an OCR model on the ORAND-CAR-A dataset, part of the HDSRC 2014 competition on handwritten strings [6]. This dataset consists of 5793 images from real bank checks taken from a Uruguayan bank. Each image contains between 2 and 8 numeric characters.

The LSTM model. We implement the OCR model described in [22], which consists of a convolutional layer, followed by a 3-layer deep bidirectional LSTM, and optimizes for CTC loss. The trained model achieves a precision score of 85.7% on the test set of ORAND-CAR-A, which would have achieved first place in the HDSRC 2014 competition.

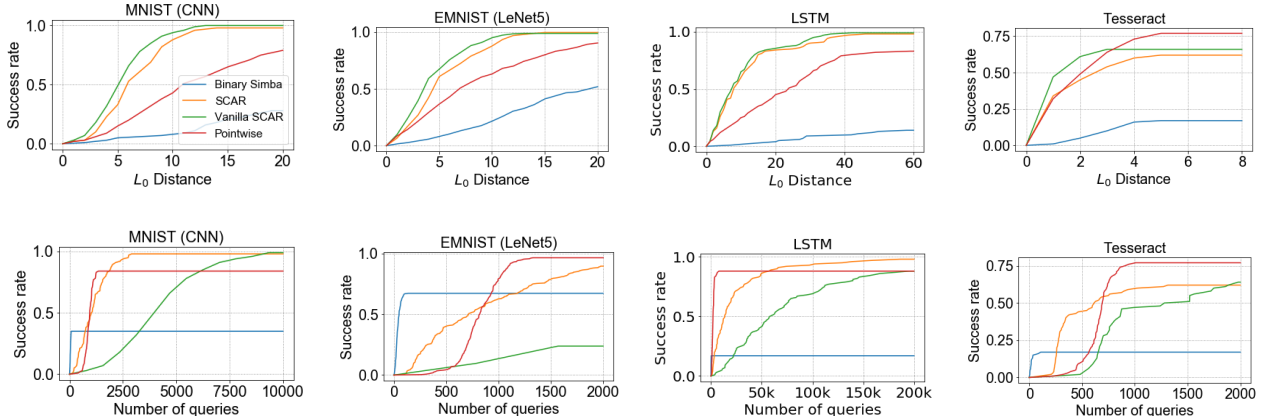


Figure 2: Success rate by L_0 distance and by number of queries for a CNN model on MNIST, a LeNet5 model on EMNIST, an LSTM model on handwritten numbers, and the Tesseract model over printed words.

Results. The results are similar to the attacks on the CNN-MNIST model. SIMBA has a less than 20 percent success rate. POINTWISE obtains a high success rate with a small number of queries, but is outperformed by SCAR and VANILLA-SCAR in terms of L_0 distance. Due to the images being high-dimensional ($d \approx 50,000$) and consisting of multiple digits, the reason why SIMBA performs poorly is because the flipped pixels are spread out over the different digits (see Figure 1).

6.4 Tesseract on printed words

We show that the vulnerability of OCR systems concerns not only handwritten text, but also printed text, which one might expect to be more robust. We explore this vulnerability in the context of English words and show that in many cases, a change in a single pixel suffices for a word to be misclassified as another word in the English dictionary.

The Tesseract model. Tesseract is a popular open-source text recognition system that is sponsored by Google [27]. We used Tesseract version 4.1.1 trained for the English language. Tesseract 4 is based on an LSTM model (see [28] for a detailed description of the architecture of Tesseract’s model). We note that Tesseract is designed for printed text, rather than handwritten.

The dataset. We attack 100 images of single printed English words that consist of four characters (the full list of words, together with the labels of the attacked images, can be found in the appendix), chosen randomly among those correctly classified by Tesseract, which has 96.5% accuracy rate. For some attacked images with a lot of noise, Tesseract does not recognize any word and rejects the input. Since the goal of these attacks is to misclassify images as words with a different meaning, we only consider an attack to be successful if the adversarial image produced is classified as a word in the English dictionary. For example, consider an attacked image of the word “one”. If Tesseract does not recognize any word in this image, or recognizes “oe” or “:one”, we do not count this image as a successful attack.

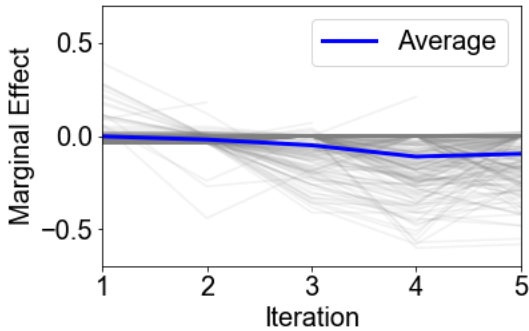


Figure 3: The gain from each pixel for the five iterations it took to successfully attack the word “idle” on Tesseract.

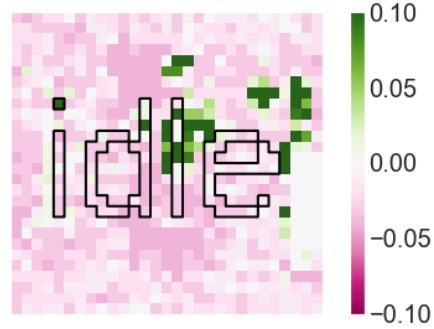


Figure 4: Heatmap of the gains from flipping a pixel on the word “idle” with Tesseract.

Results. The main result for the attacks on Tesseract is that, surprisingly, for around half of the images, flipping a *single* pixel results in the image being classified as a different word in the English dictionary (see Figure 2). SCAR again produces attacks with L_0 distance close to VANILLA-SCAR, but with fewer queries. Unlike the other models, SCAR and VANILLA-SCAR do not reach close to 100% accuracy rate. We hypothesize that this is due to the fact that, unlike digits, not every combination of letters forms a valid label, so many words have an edit distance of multiple characters to get to the closest different label. In these experiments, POINTWISE obtains the highest success rate.

Spatial and temporal correlations. As discussed in Section ??, SCAR exploits spatial and temporal correlations to optimize the number of queries needed. As an example, we consider SCAR attacking Tesseract on the word “idle”.

In Figure 3 we plot a separate line for each pixel p and the corresponding decrease in confidence from flipping that pixel at each iteration. We first note the pixels with the smallest gains at some iteration are often among the pixels with the smallest gains in the next iteration, which indicates temporal correlations. Most of the gains are negative, which implies that, surprisingly, for most pixels, flipping that pixel *increases* the confidence of the true label. Thus, randomly choosing which pixel to flip, as in SIMBA, is ineffective.

Figure 4 again shows the gain from flipping each pixel, but this time as a heatmap for the gains at the first iteration. We note that most pixels with a large gain have at least one neighboring pixel that also has a large gain. This heatmap illustrates that first querying the neighboring pixels of the previous pixel flipped is an effective technique to reduce the number of queries needed to find a high gain pixel.

6.5 Check processing systems

We licensed software from providers of check processing systems to major US banks and applied the attack described in Algorithm 3. This software includes the prediction confidence as part of their output. Naturally, access to these systems is limited and the cost per query is significant. We confirm the findings from the previous experiments that SCAR, which is used as a subroutine by

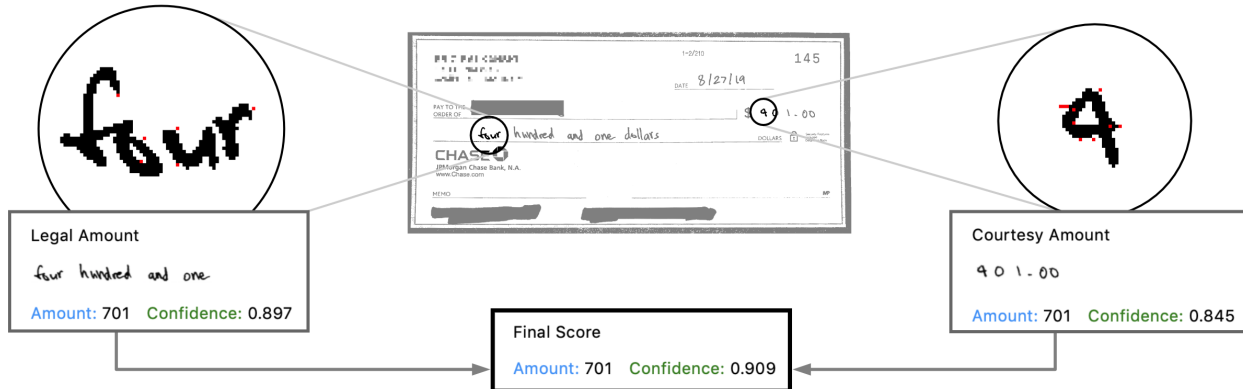


Figure 5: An example of a check for \$401 attacked by Algorithm 3 that is misclassified with high confidence as \$701 by a check processing system used by US banks.

Algorithm 3, is effective in query-limited settings and showcase the vulnerability of OCR systems used in the industry. Check fraud is a major concern for US banks; it caused over \$1.3 billion in losses in 2018 [2].

We obtained a 17.1% success rate (19 out of 111 checks) when attacking check processing systems used by banks for mobile check deposits. As previously mentioned, a check is successfully attacked when both amounts on the check are misclassified as the same wrong amount (see Figure 5). Since check fraud occurs at large scale, we believe that this vulnerability raises serious concerns.¹

Classifier	Queries	L_0 distance
CAR (F_C)	1615	11.77
LAR (F_L)	8757	14.85

Table 2: Average number of queries and L_0 distance on the CAR and LAR classifiers for the high confidence successful attacks.

We say that a check is misclassified with high confidence if the amounts written in number and words are each classified with confidence at least 50% for the wrong label. We obtained high confidence misclassification for 76.5% of the checks successfully attacked. In Figure 5, we show the output of a check for \$401 that has both amounts classified as 701 with confidence at least 80%. On average, over the checks for which we obtained high confidence misclassification, Algorithm 3 flipped 11.77 and 14.85 pixels and made 1615 and 8757 queries for the amounts in numbers and words respectively. The checks are high resolution, with widths of size 1000. Additional examples of checks misclassified with high confidence can be found in the appendix.

¹Regarding physical realizability: instead of printing an adversarial check in high resolution, an attacker can redirect the camera input of a mobile phone to arbitrary image files, which avoids printing and taking a picture of an adversarial check. This hacking of the camera input is easy to perform on Android.

References

- [1] Abdullah Al-Dujaili and Una-May O’Reilly. There are no bit parts for sign bits in black-box attacks. *arXiv preprint arXiv:1902.06894*, 2019.
- [2] American Bankers Association. Deposit account fraud survey. 2020. URL <https://www.aba.com/news-research/research-analysis/deposit-account-fraud-survey-report>.
- [3] Nicholas Carlini and David Wagner. Towards evaluating the robustness of neural networks. In *2017 IEEE symposium on security and privacy (SP)*, pages 39–57. IEEE, 2017.
- [4] Pin-Yu Chen, Huan Zhang, Yash Sharma, Jinfeng Yi, and Cho-Jui Hsieh. Zoo: Zeroth order optimization based black-box attacks to deep neural networks without training substitute models. In *Proceedings of the 10th ACM Workshop on Artificial Intelligence and Security*, pages 15–26, 2017.
- [5] Gregory Cohen, Saeed Afshar, Jonathan Tapson, and Andre Van Schaik. EMNIST: Extending MNIST to handwritten letters. In *2017 International Joint Conference on Neural Networks (IJCNN)*, pages 2921–2926. IEEE, 2017.
- [6] Markus Diem, Stefan Fiel, Florian Kleber, Robert Sablatnig, Jose M Saavedra, David Contreras, Juan Manuel Barrios, and Luiz S Oliveira. ICFHR 2014 competition on handwritten digit string recognition in challenging datasets (HDSRC 2014). In *2014 14th International Conference on Frontiers in Handwriting Recognition*, pages 779–784. IEEE, 2014.
- [7] Gavin Weiguang Ding, Kry Yik Chau Lui, Xiaomeng Jin, Luyu Wang, and Ruitong Huang. On the sensitivity of adversarial robustness to input data distributions. In *ICLR (Poster)*, 2019.
- [8] Ian J Goodfellow, Jonathon Shlens, and Christian Szegedy. Explaining and harnessing adversarial examples. *arXiv preprint arXiv:1412.6572*, 2014.
- [9] Chuan Guo, Jacob R Gardner, Yurong You, Andrew Gordon Wilson, and Kilian Q Weinberger. Simple black-box adversarial attacks. *arXiv preprint arXiv:1905.07121*, 2019.
- [10] Maya R Gupta, Nathaniel P Jacobson, and Eric K Garcia. OCR binarization and image pre-processing for searching historical documents. *Pattern Recognition*, 40(2):389–397, 2007.
- [11] Andrew Ilyas, Logan Engstrom, Anish Athalye, and Jessy Lin. Black-box adversarial attacks with limited queries and information. *arXiv preprint arXiv:1804.08598*, 2018.
- [12] Andrew Ilyas, Logan Engstrom, and Aleksander Madry. Prior convictions: Black-box adversarial attacks with bandits and priors. *arXiv preprint arXiv:1807.07978*, 2018.
- [13] R Jayadevan, Satish R Kolhe, Pradeep M Patil, and Umapada Pal. Automatic processing of handwritten bank cheque images: a survey. *International Journal on Document Analysis and Recognition (IJDAR)*, 15(4):267–296, 2012.
- [14] Alexey Kurakin, Ian Goodfellow, and Samy Bengio. Adversarial examples in the physical world. *arXiv preprint arXiv:1607.02533*, 2016.

- [15] Yann LeCun, Léon Bottou, Yoshua Bengio, and Patrick Haffner. Gradient-based learning applied to document recognition. *Proceedings of the IEEE*, 86(11):2278–2324, 1998.
- [16] Yann LeCun, Corinna Cortes, and CJ Burges. MNIST handwritten digit database. 2010.
- [17] Qi Lei, Lingfei Wu, Pin-Yu Chen, Alexandros G Dimakis, Inderjit S Dhillon, and Michael Witbrock. Discrete adversarial attacks and submodular optimization with applications to text classification. *arXiv preprint arXiv:1812.00151*, 2018.
- [18] Yandong Li, Lijun Li, Liqiang Wang, Tong Zhang, and Boqing Gong. Nattack: Learning the distributions of adversarial examples for an improved black-box attack on deep neural networks. *arXiv preprint arXiv:1905.00441*, 2019.
- [19] Aleksander Madry, Aleksandar Makelov, Ludwig Schmidt, Dimitris Tsipras, and Adrian Vladu. Towards deep learning models resistant to adversarial attacks. *arXiv preprint arXiv:1706.06083*, 2017.
- [20] Seungyong Moon, Gaon An, and Hyun Oh Song. Parsimonious black-box adversarial attacks via efficient combinatorial optimization. *arXiv preprint arXiv:1905.06635*, 2019.
- [21] Seyed-Mohsen Moosavi-Dezfooli, Alhussein Fawzi, and Pascal Frossard. Deepfool: a simple and accurate method to fool deep neural networks. In *Proceedings of the IEEE conference on computer vision and pattern recognition*, pages 2574–2582, 2016.
- [22] Noam Mor and Lior Wolf. Confidence prediction for lexicon-free OCR. In *2018 IEEE Winter Conference on Applications of Computer Vision (WACV)*, pages 218–225. IEEE, 2018.
- [23] Nicolas Papernot, Patrick McDaniel, Somesh Jha, Matt Fredrikson, Z Berkay Celik, and Ananthram Swami. The limitations of deep learning in adversarial settings. In *2016 IEEE European symposium on security and privacy (EuroS&P)*, pages 372–387. IEEE, 2016.
- [24] Jonas Rauber, Wieland Brendel, and Matthias Bethge. Foolbox: A python toolbox to benchmark the robustness of machine learning models. *arXiv preprint arXiv:1707.04131*, 2017.
- [25] Ludwig Schmidt, Shibani Santurkar, Dimitris Tsipras, Kunal Talwar, and Aleksander Madry. Adversarially robust generalization requires more data. In *Advances in Neural Information Processing Systems*, pages 5014–5026, 2018.
- [26] Lukas Schott, Jonas Rauber, Matthias Bethge, and Wieland Brendel. Towards the first adversarially robust neural network model on MNIST. *arXiv preprint arXiv:1805.09190*, 2018.
- [27] Ray Smith. An overview of the Tesseract OCR engine. In *Ninth International Conference on Document Analysis and Recognition (ICDAR 2007)*, volume 2, pages 629–633. IEEE, 2007.
- [28] Congzheng Song and Vitaly Shmatikov. Fooling OCR systems with adversarial text images. *arXiv preprint arXiv:1802.05385*, 2018.
- [29] Christian Szegedy, Wojciech Zaremba, Ilya Sutskever, Joan Bruna, Dumitru Erhan, Ian Goodfellow, and Rob Fergus. Intriguing properties of neural networks. *arXiv preprint arXiv:1312.6199*, 2013.

- [30] Chun-Chen Tu, Paishun Ting, Pin-Yu Chen, Sijia Liu, Huan Zhang, Jinfeng Yi, Cho-Jui Hsieh, and Shin-Ming Cheng. Autozoom: Autoencoder-based zeroth order optimization method for attacking black-box neural networks. In *Proceedings of the AAAI Conference on Artificial Intelligence*, volume 33, pages 742–749, 2019.

Appendix

A Missing analysis from Section 3

Theorem 1. *There exists an m -class linear classifier F for d -dimensional binary images s.t. for all classes i , there exists at least one binary image \mathbf{x} in i that is robust to $d/4 - \sqrt{2d \log m}/2$ pixel changes, i.e., for all \mathbf{x}' s.t. $\|\mathbf{x} - \mathbf{x}'\|_0 \leq d/4 - \sqrt{2d \log m}/2$, $\arg \max_j F(\mathbf{x}')_j = i$.*

Proof. In this proof, we assume that binary images have pixel values in $\{-1, 1\}$ instead of $\{0, 1\}$. We consider a linear classifier $F_{\mathbf{w}_1^*, \dots, \mathbf{w}_m^*}$ such that the predicted label y of a binary image \mathbf{x} is $y = \arg \max_i \mathbf{x}^\top \mathbf{w}_i^*$.

We wish to show the existence of weight vectors $\mathbf{w}_1^*, \dots, \mathbf{w}_m^*$ that all have large pairwise L_0 distance. This is closely related to error-correction codes in coding theory which, in order to detect and reconstruct a noisy codes, also aims to construct binary codes with large pairwise distance.

We do this using the probabilistic method. Consider m binary weight vectors $\mathbf{w}_1, \dots, \mathbf{w}_m$ chosen uniformly at random, and independently, among all d -dimensional binary vectors $\mathbf{w} \in \{-1, 1\}^d$. By the Chernoff bound, for all $i, j \in [m]$, we have that for $0 < \delta < 1$,

$$\Pr[\|\mathbf{w}_i - \mathbf{w}_j\|_0 \leq (1 - \delta)d/2] \leq e^{-\delta^2 d/4}.$$

There are $\binom{m}{2} < m^2$ pairs of images (i, j) . By a union bound and with $\delta = \sqrt{8 \log m/d}$, we get that

$$\Pr\left[\|\mathbf{w}_i - \mathbf{w}_j\|_0 > d/2 - \sqrt{2d \log m} : \text{for all } i, j \in [m], i \neq j\right] > 1 - m^2 e^{-\delta^2 d/4} > 0.$$

Thus, by the probabilistic method, there exists $\mathbf{w}_1^*, \dots, \mathbf{w}_m^*$ such that $\|\mathbf{w}_i^* - \mathbf{w}_j^*\|_0 > d/2 - \sqrt{2d \log m}$ for all $i, j \in [m]$.

It remains to show that the linear classifier $F_{\mathbf{w}_1^*, \dots, \mathbf{w}_m^*}$ satisfies the condition of the theorem statement. For class i , consider the binary image $\mathbf{x}_i = \mathbf{w}_i^*$. Note that for binary images $\mathbf{x} \in \{-1, 1\}^d$, we have $\mathbf{x}^\top \mathbf{w}_i^* = d - 2\|\mathbf{x} - \mathbf{w}_i^*\|_0$. Thus, $\mathbf{x}_i^\top \mathbf{w}_i^* = d$ and $\arg \max_{j \neq i} \mathbf{x}_i^\top \mathbf{w}_j^* < 2\sqrt{2d \log m}$, and we get $\mathbf{x}_i^\top \mathbf{w}_i^* - \arg \max_{j \neq i} \mathbf{x}_i^\top \mathbf{w}_j^* > d - 2\sqrt{2d \log m}$. Each pixel change reduces this difference by at most 4. Thus, for all \mathbf{x}' such that $\|\mathbf{x}_i - \mathbf{x}'\|_0 \leq (d - 2\sqrt{2d \log m})/4 = d/4 - \sqrt{2d \log m}/2$, we have $\mathbf{x}'^\top \mathbf{w}_i^* - \arg \max_{j \neq i} \mathbf{x}'^\top \mathbf{w}_j^* > 0$ and the predicted label of \mathbf{x}' is i . \square

Theorem 2. *There exists a 2-class linear classifier F for d -dimensional binary images such that for both classes i , a uniformly random binary image \mathbf{x} in that class i is robust to $\sqrt{d}/8$ pixel changes in expectation, i.e. $\mathbb{E}_{\mathbf{x} \sim \mathcal{U}(i)}[\min_{\mathbf{x}' : \arg \max_j F(\mathbf{x}')_{j \neq i}} \|\mathbf{x} - \mathbf{x}'\|_0] \geq \sqrt{d}/8$.*

Proof. Consider the following linear classifier

$$F(\mathbf{x}) = \begin{cases} 0 & \text{if } \bar{1}^\top \vec{x} - x_0/2 < \frac{d}{2} \\ 1 & \text{otherwise} \end{cases}.$$

Informally, this is a classifier which assigns label 0 if $\|\mathbf{x}\|_0 < d/2$ and label 1 if $\|\mathbf{x}\|_0 > d/2$. The classifier tiebreaks the $\|\mathbf{x}\|_0 = d/2$ case depending on whether or not the first position in \mathbf{x} is a 1 or a 0. Notice that this classifier assigns exactly half the space the label 0, and the other half the label 1.

Consider class 0 and let $\mathcal{U}(0)$ be the uniform distribution over all \mathbf{x} in class 0. We have

$$\Pr_{\mathbf{x} \in \mathcal{U}(0)} [\|\mathbf{x}\|_0 = s] = \frac{1}{2^d} \binom{d}{s}$$

when $s < d/2$ and $\Pr_{\mathbf{x} \in \mathcal{U}(0)} [\|\mathbf{x}\|_0 = s] = \frac{1}{2^{d+1}} \binom{d}{s}$ when $s = d/2$. The binomial coefficient $\binom{d}{s}$ is maximized when $s = d/2$. For all $d \in \mathbb{Z}^+$, Stirling's approximation gives lower and upper bounds of $\sqrt{2\pi}d^{d+\frac{1}{2}}e^{-d} \leq d! \leq d^{d+\frac{1}{2}}e^{-d+1}$. Since d is even, we get

$$\binom{d}{d/2} = \frac{d!}{(\frac{d}{2}!)^2} \leq \frac{e2^d}{\pi\sqrt{d}}.$$

Therefore, we have that for all s ,

$$\Pr_{\mathbf{x} \in \mathcal{U}(0)} [\|\mathbf{x}\|_0 = s] \leq \frac{1}{2^d} \binom{d}{d/2} \leq \frac{e2^d}{\pi\sqrt{d}},$$

which implies

$$\Pr_{\mathbf{x} \in \mathcal{U}(0)} \left[\left| \|\mathbf{x}\|_0 - d/2 \right| \geq \frac{\pi\sqrt{d}}{4e} \right] \geq 1 - \frac{2\pi\sqrt{d}}{4e} \cdot \frac{e}{\pi\sqrt{d}} = \frac{1}{2}.$$

The same argument follows similarly for members of class 1. Therefore, for either class, at least half of the images \vec{x} of that class are such that $|\|\mathbf{x}\|_0 - d/2| \geq \frac{\pi\sqrt{d}}{4e} \geq \frac{\sqrt{d}}{4}$. These images require at least $\frac{\sqrt{d}}{4}$ pixel flips in order to change the predicted label according to F , and we obtain the bound in the theorem statement. \square

B Additional Description of Datasets and Models

B.1 Digit and character recognition systems

The datasets. We preprocess the EMNIST letter dataset to only include lowercase letters, since an uppercase letter which is misclassified as the corresponding lowercase letter does not change the semantic meaning of the overall word. We randomly select 10 correctly-classified samples from each class in MNIST and EMNIST lowercase letters to form two datasets to attack.

Models. We consider the following five models, trained in the same manner for the MNIST and EMNIST datasets. For each model, we also list their Top-1 accuracies on MNIST and EMNIST.

- **LogReg:** We create a logistic regression model by flattening the input and follow this with a fully connected layer with softmax activation. (MNIST: 91.87% / EMNIST: 80.87%)
- **MLP2:** We create a 2-layer MLP by flattening the input, followed by two sets of fully connected layers of size 512 with ReLU activation and dropout rate 0.2. We then add a fully connected layer with softmax activation. (MNIST: 98.01% / EMNIST: 93.46%)
- **CNN:** We use two convolutional layers of 32 and 64 filters of size 3×3 , each with ReLU activation. The latter layer is followed by a 2×2 Max Pooling layer with dropout rate 0.25. (MNIST: 99.02% / EMNIST: 95.04%)

This output is flattened and followed by a fully connected layer of size 128 with ReLU activation and dropout rate 0.5. We then add a fully connected layer with softmax activation.

- **LeNet 5:** We use the same architecture as in [15]. (MNIST: 99.01% / EMNIST: 94.33%)
- **SVM:** We use the `sklearn` implementation with default parameters. (MNIST: 94.11% / EMNIST: 87.53%)

Except for the SVM, we train each model for 50 epochs with batch size 128, using the Adam optimizer with a learning rate of 10^{-3} . The experimental results for CNN on MNIST and LeNet5 on EMNIST are shown in Section 5.

B.2 LSTM on handwritten numbers

The dataset. We train an OCR model on the ORAND-CAR-A dataset, part of the HDSRC 2014 competition on handwritten strings [6]. This dataset consists of 5793 images from real bank checks taken from a Uruguayan bank. The characters in these images consist of numeric characters (0-9) and each image contains between 2 and 8 characters. These images also contain some background noise due to the real nature of the images. We observe the train/test split given in the initial competition, meaning that we train our model on 2009 images and attack only a randomly selected subset from the test set (another 3784 images). The images as presented in the competition were colored, but we binarize them in a similar preprocessing step as done for MNIST/EMNIST datasets.

The LSTM model. We implement the OCR model described in [22], which consists of a convolutional layer, followed by a 3-layer deep bidirectional LSTM, and optimizes for CTC loss. CTC decoding was done using a beam search of width 100. The model was trained with the Adam optimizer using a learning rate of 10^{-4} , and was trained for 50 epochs. The trained model achieves a precision score of .857 on the test set of ORAND-CAR-A, which would have achieved first place in that competition.

B.3 Tesseract on printed words

The model. We use Tesseract version 4.1.1 trained for the English language. Tesseract 4 is based on an LSTM model (see [28] for a detailed description of the architecture of Tesseract’s model).

The dataset. We attack images of a single printed English word. Tesseract supports a large number of languages, and we use the version of Tesseract trained for the English language. We picked words of length four in the English dictionary. We then rendered these words in black over a white background using the Arial font in size 15. We added 10 white pixels for padding on each side of the word. The accuracy rate over 1000 such images of English words of length four chosen at random is 0.965 and the average confidence among words correctly classified is 0.906. Among the words correctly classified by Tesseract, we selected 100 at random to attack.

For some attacked images with a lot of noise, Tesseract does not recognize any word and rejects the input. Since the goal of these attacks is to misclassify images as words with a different meaning, we only consider an attack to be successful if the adversarial image produced is classified as a word in the English dictionary. For example, consider an attacked image of the word “one”. If Tesseract does not recognize any word in this image, or recognizes “oe” or “:one”, we do not count this image as a successful attack.

We restricted the attacks to pixels that were at distance at most three of the box around the word. Since our algorithm only considers boundary pixels, this restriction avoids giving an unfair

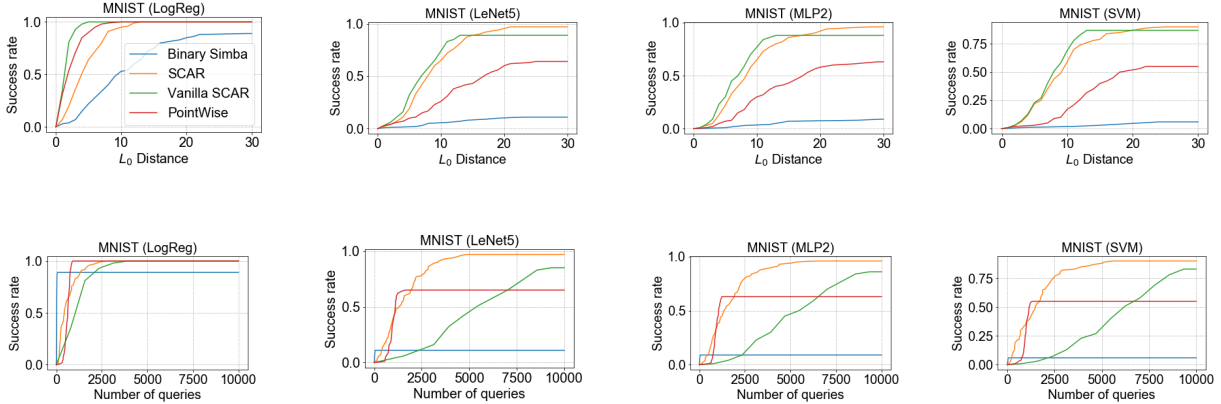


Figure 6: Success rate by L_0 distance and by number of queries for four different models on MNIST.

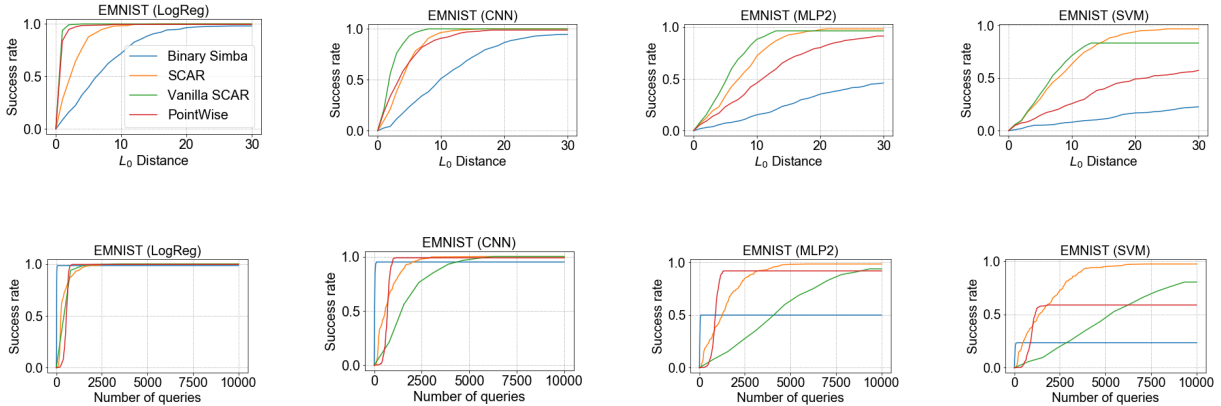


Figure 7: Success rate by L_0 distance and by number of queries for four different models on EMNIST.

advantage to our algorithm in terms of total number of queries. In some cases, especially images with a lot of noise, Tesseract does not recognize any word and rejects the input. Since the goal of these attacks is to misclassify images as words with a different meaning than the true word, we only consider an attack to be successful if the adversarial image produced is classified as a word in the English dictionary. For example, consider an image with the text “one”. If Tesseract does not recognize any word in this image, or recognizes “oe” or “:one”, we do not count this image as a successful attack.



Figure 8: Examples of attacks on the LSTM for handwritten numbers. The images correspond to, from left to right, the original image, the outputs of SCAR, VANILLA-SCAR, POINTWISE, and SIMBA.

C Additional Experimental Results

In Figure 6 and Figure 7, we provide additional experimental results on the MNIST and EMNIST datasets. In Figure 8, we give additional examples of attacks on the LSTM model for handwritten number. In Table 1, we list the 100 English words of length 4 we attacked together with the word label of the image resulting from running SCAR.

Finally, in Figure 6, we show additional examples of our attacks on check processing systems.



Figure 9: First digit and word of the CAR and LAR amount of checks for \$562, \$72, and \$2 misclassified as \$862, \$92, and \$3 by a check processing system. The pixels in red correspond to pixels whose colors differ between the original and attacked image.

Original word	Label from Scar		Original word	Label from Scar		Original word	Label from Scar
down	dower		race	rate		punt	pant
fads	fats		nosy	rosy		mans	mans
pipe	pie		serf	set		cram	ram
soft	soft		dare	dare		cape	tape
pure	pure		hood	hoot		bide	hide
zoom	zoom		yarn	yam		full	fall
lone	tone		gorp	gore		lags	fags
fuck	fucks		fate	ate		dolt	dot
fist	fist		mags	mays		mods	mots
went	weal		oust	bust		game	game
omen	men		rage	rage		taco	taco
idle	die		moth	math		ecol	col
yeah	yeah		woad	woad		deaf	deaf
feed	feet		aged	ed		vary	vary
nuns	runs		dray	ray		tell	tel
educ	educ		ency	ency		avow	vow
gush	gust		pres	press		wits	wits
news	news		deep	sleep		weep	ween
swim	swim		bldg	bid		vile	vie
hays	nays		warp	war		sets	nets
tube	lube		lost	lo		smut	snout
lure	hare		sqrt	sat		mies	miles
romp	romp		okay	okay		boot	hoot
comp	camp		kept	sept		yipe	vie
pith	pithy		herb	herbs		hail	fail
ploy	pro		show	how		saga	gaga
toot	foot		hick	nick		drat	rat
boll	boil		tout	foul		limo	lino
elev	ale		blur	bur		idem	idler
dank	dank		biog	dog		twinn	twins
gild	ail		lain	fain		slip	sip
waxy	waxy		gens	gents		yeti	yet
test	fest		mega	mega		loge	toge
pups	pups						

Table 3: The 100 English words of length 4 we attacked together with the word label of the image resulting from running SCAR.